Cell Reports
Report

Cell PRESS
Open ACCESS

Staufen2 Regulates Neuronal Target RNAs

Jacki E. Heraud-Farlow,[1,10] Tejaswini Sharangdhar,[2] Xiao Li,[3,4] Philipp Pfeifer,[1] Stefanie Tauber,[5,11] Denise Orozco,[6,8] Alexandra Hörmann,[1] Sabine Thomas,[1,2] Anetta Bakosova,[1] Ashley R. Farlow,[7] Dieter Edbauer,[6,8,9] Howard D. Lipshitz,[3] Quaid D. Morris,[3,4] Martin Bilban,[5] Michael Doyle,[1,*] and Michael A. Kiebler[1,2,*]

[1]Department of Neuronal Cell Biology, Center for Brain Research, 1090 Vienna, Austria
[2]Department of Anatomy and Cell Biology, Ludwig-Maximilians-University, 80336 Munich, Germany
[3]Department of Molecular Genetics, University of Toronto, Toronto, ON M5S 1A8, Canada
[4]The Donnelly Centre, University of Toronto, Toronto, ON M5S 1E3, Canada
[5]Department of Laboratory Medicine and Core Facility Genomics, Medical University of Vienna, 1090 Vienna, Austria
[6]Adolf Butenandt Institute, Ludwig-Maximilians-University, 80336 Munich, Germany
[7]Gregor Mendel Institute of Molecular Plant Biology, Austrian Academy of Sciences, 1030 Vienna, Austria
[8]German Center for Neurodegenerative Diseases (DZNE), 80336 Munich, Germany
[9]Munich Cluster of Systems Neurology (SyNergy), 80336 Munich, Germany
[10]Department of Chromosome Biology, Max F. Perutz Laboratories, University of Vienna, 1030 Vienna, Austria
[11]Present address: Center for Integrative Bioinformatics Vienna, Max F. Perutz Laboratories, University of Vienna, 1030 Vienna, Austria
*Correspondence: michael.kiebler@med.uni-muenchen.de (M.A.K.), michael.doyle@meduniwien.ac.at (M.D.)
http://dx.doi.org/10.1016/j.celrep.2013.11.039
This is an open-access article distributed under the terms of the Creative Commons Attribution-NonCommercial-No Derivative Works License, which permits non-commercial use, distribution, and reproduction in any medium, provided the original author and source are credited.

SUMMARY

RNA-binding proteins play crucial roles in directing RNA translation to neuronal synapses. Staufen2 (Stau2) has been implicated in both dendritic RNA localization and synaptic plasticity in mammalian neurons. Here, we report the identification of functionally relevant Stau2 target mRNAs in neurons. The majority of Stau2-copurifying mRNAs expressed in the hippocampus are present in neuronal processes, further implicating Stau2 in dendritic mRNA regulation. Stau2 targets are enriched for secondary structures similar to those identified in the 3′ UTRs of *Drosophila* Staufen targets. Next, we show that Stau2 regulates steady-state levels of many neuronal RNAs and that its targets are predominantly downregulated in Stau2-deficient neurons. Detailed analysis confirms that Stau2 stabilizes the expression of one synaptic signaling component, the regulator of G protein signaling 4 (*Rgs4*) mRNA, via its 3′ UTR. This study defines the global impact of Stau2 on mRNAs in neurons, revealing a role in stabilization of the levels of synaptic targets.

INTRODUCTION

In neurons, RNA-binding proteins (RBPs) are essential for directing gene expression to distinct regions of the cell, such as growth cones or synapses (Holt and Bullock, 2009). Local protein synthesis in neuronal dendrites and at synapses is critically important for both synaptic development and plasticity (Costa-Mattioli et al., 2009; Sutton and Schuman, 2006; Kandel, 2009). Staufen proteins are double-stranded RBPs (dsRBP) involved in RNA localization and synaptic plasticity (Dubnau et al., 2003; Lebeau et al., 2011; St Johnston et al., 1991). Work in several organisms indicates a role in RNA transport, stability, translation, and anchoring (Dugré-Brisson et al., 2005; Kim et al., 2005; Micklem et al., 2000; Tang et al., 2001; Zimyanin et al., 2008). However, Staufen's role in RNA localization in neurons is not well understood.

Staufen2 (Stau2) is highly enriched in the brain and is important for dendritic spine morphogenesis, which represent excitatory synapses (Goetze et al., 2006). It is viewed as one of the best markers to follow the transport of RNPs due to its fast bidirectional movement along dendritic microtubules (Köhrmann et al., 1999; Zimyanin et al., 2008). Supporting its role in RNA localization, expression of a dominant-negative Stau2 relocalizes a large proportion of total dendritic RNA toward the cell body (Tang et al., 2001). Furthermore, downregulation of Stau2 in neurons impairs metabotropic glutamate receptor (mGluR)-dependent long-term depression (LTD) (Lebeau et al., 2011).

Outstanding questions regarding the role of Stau2 in mature neurons include which mRNAs it interacts with and whether it plays a role in regulating their expression or localization. Here, we sought to globally identify which mRNAs are associated with Stau2 protein in the brain and investigate their regulation. We report that Stau2 modulates the expression—most notably the stabilization—of a subset of target RNAs that encode synaptic proteins. These targets are enriched for a recently identified RNA secondary structure bound by *Drosophila* Staufen (Laver et al., 2013). In conclusion, our data identify a mechanism for Stau2 regulation of synaptic targets in neurons.

RESULTS

Identification of Stau2 Target RNAs from Rodent Brain

To isolate Stau2-containing RNA granules not linked to membranes, we developed a protocol for RNP purification (Fritzsche

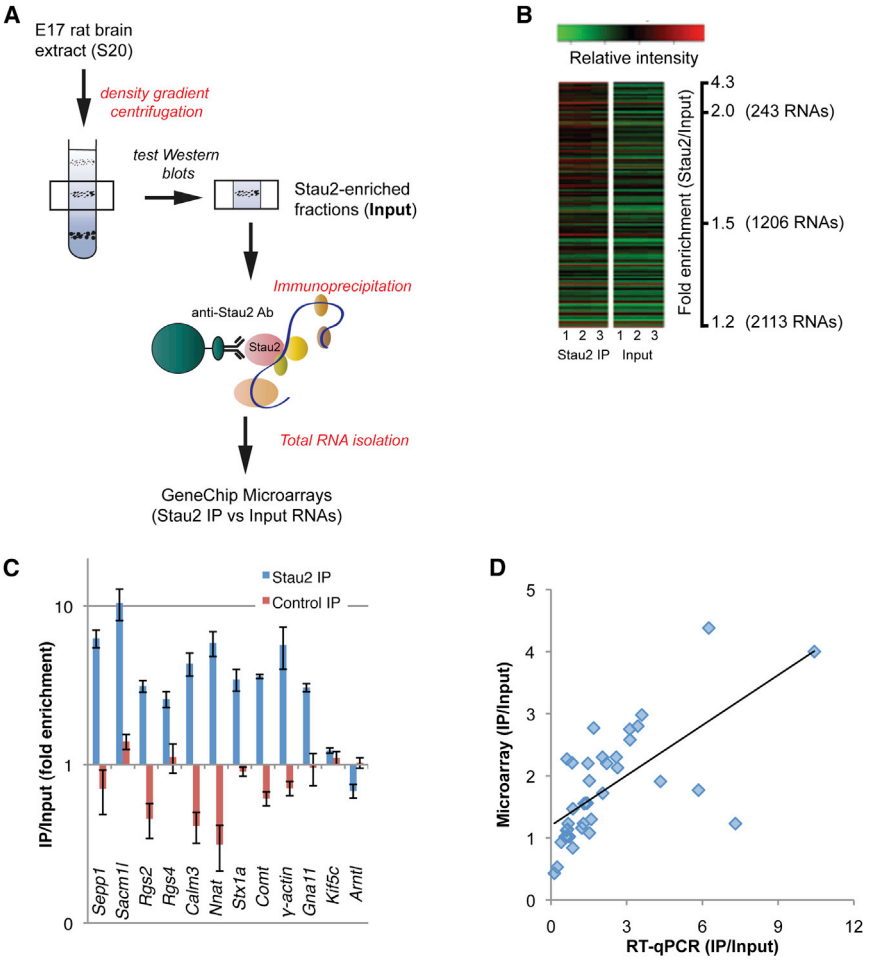

E

Term	No. of RNAs	*P*-value (BH)	Enrichment
Protein localization	82	5.4E-10	2.39
Small GTPase mediated signal transduction	43	3.4E-10	3.61
Mitochondrion	115	6.5E-06	1.62
Intracellular signaling cascade	83	4.1E-04	1.72
ARF/SAR superfamily	10	4.7E-03	5.95

Figure 1. Identification of Stau2 Target RNAs from Soluble Stau2 RNPs

(A) The three-step biochemical procedure to isolate endogenous Stau2 RNPs and identify their RNA content.

(B) Heatmap of Affymetrix GeneChip arrays showing the relative intensity of significantly enriched genes (adjusted p value < 0.05) in the Stau2 IP compared to the input from three independent experiments. Each row represents a single mRNA.

(C) Validation of microarrays by qRT-PCR. mRNA was isolated from input, Stau2 IPs, control IPs (using rabbit preimmune sera), and the candidate target genes quantified by qRT-PCR. Enrichment was calculated as the IP relative to input and cross-normalized to the reference genes *Kif5c* and *Arntl*. The mean ± SEM is shown ($n \geq 3$).

(D) Correlation of enrichment values (Stau2 IP/input) obtained by microarray versus qRT-PCR. Each point represents an individual mRNA, which was quantified using both methods ($n \geq 2$). Pearson's correlation coefficient was significant ($p < 0.0001$).

(E) Selected GO term enrichments observed for Stau2-associated mRNAs. RNAs enriched ≥1.5-fold (Stau2 IP/input) were used (n = 1,113).

See also Figure S1 and Tables S1 and S2.

et al., 2013) (Figure 1A). Soluble (S20) embryonic day 17 (E17) rat brain preparations were separated by density gradient centrifugation. Western blotting was used to identify those fractions that were enriched for Stau2 but depleted of endoplasmic reticulum (ER). Fractionation before immunoprecipitation (IP) greatly reduces nonspecific interactors, as the ER is associated with ribosomes and translating RNAs.

Affinity-purified monospecific Stau2 antibodies coupled to protein A beads were used to isolate endogenous RNPs from ER-depleted brain fractions. In three independent experiments, total RNA was isolated from the IP and analyzed by microarray. Equal amounts of IP and input RNA were hybridized to the array and the identified RNAs were ranked by enrichment in the IP relative to input (Table S1). This identified a total of 1,206 RNAs significantly enriched in the Stau2 IP (using an average of >1.5-fold enrichment as a cutoff across three IPs and an adjusted p value < 0.05; Figure 1B). This represents ~8.5% of mRNAs expressed in the input fractions. The enrichment of 38 candidate RNAs from independent IPs was confirmed by quantitative RT-PCR (qRT-PCR) (Figure 1C; Table S2). The candidates included RNAs with a range of enrichments and abundance to ensure that all classes of RNAs could be validated. Preimmune serum coupled to protein A beads was used as a negative control (Figure 1C). Note that the preimmune IPs could not be used as a control for the microarrays because insufficient RNA was isolated. The correlation between qRT-PCR and microarray data for the selected 38 genes was highly significant (Pearson's correlation coefficient, p < 0.0001; Figure 1D), indicating that the microarray data are robust and reliable. As an independent control, we tested whether candidate RNAs were enriched in the IP of another RBP, Barentsz (Btz), which forms distinct RNPs compared to Stau2 in neurons (Fritzsche et al., 2013). Only one (*Sacm1l*) out of the six tested Stau2 target RNAs was also enriched in the Btz IP (Figure S1A). Indeed, no overlapping targets were enriched >2-fold in both IPs by microarray analysis (M.A.K., M.D., J.E.H.-F., D. Karra, P.P., S.T., and M. B., unpublished data) further suggesting that most of the identified Stau2 targets are specific to this RNP.

Increasing evidence demonstrates that individual RBPs can regulate a biologically coherent set of target RNAs and coordinate their expression (Hogan et al., 2008; Keene, 2007; Ule et al., 2005). Therefore, we performed DAVID Gene Ontology (GO) term analysis of the Stau2 targets (>1.5-fold) and identified

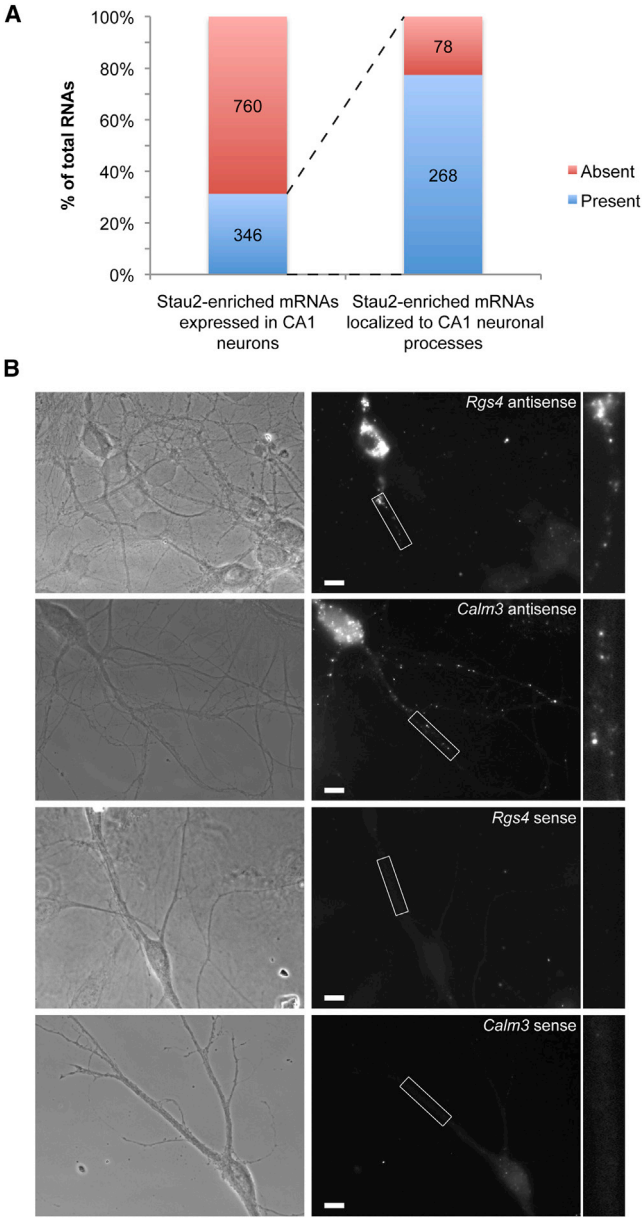

Figure 2. Most Stau2 Targets Localize to Neuronal Processes in the Hippocampus CA1 Region

(A) Stau2 targets identified in this study were compared to a new data set of process-localized mRNAs from the CA1 region of the hippocampus (Cajigas et al., 2012). The data set was derived from RNA sequencing of the soma and neuropil layers from the CA1 region of mouse hippocampus. The first column indicates the number and percentage of Stau2 target RNAs expressed in the CA1 somatic layer. The second column indicates the number and percentage of Stau2 target mRNAs that are expressed in the CA1 that are also found in the neuropil (~77%).

(B) Localization of two Stau2 target mRNAs, *Rgs4* and *Calm3*, was tested by fluorescent in situ hybridization using digoxigenin-labeled riboprobes in primary hippocampal neurons (15–16 days in vitro). Sense probes were used as negative controls. Scale bar, 10 μM.

See also Table S3.

enriched classes of genes (Huang et al., 2009). We found a significant enrichment of several GO term categories, including protein localization and signal transduction mediated by small GTPases (p values of 5.4×10^{-10} and 3.4×10^{-10}, respectively; Figure 1E). Interestingly, eight RNAs encode proteins that are part of a G protein-coupled receptor (GPCR) signaling pathway (Figure S1B). This pathway is important for signaling through synaptic receptors such as the dopamine, glutamate, and muscarinic acetylcholine receptors, among others (Lin et al., 2002; Miura et al., 2002; Rashid et al., 2007). This result raises the possibility that Stau2 may regulate RNAs encoding functionally related proteins as described for other neuronal RBPs, such as Nova and FMRP (Darnell et al., 2011; Ule et al., 2005). In support of a possible role of Stau2 in intracellular signaling cascades, we found both ERK1 and ERK2 kinases to be misregulated when Stau2 levels were reduced in primary cortical neurons (Figures S1C and S1D).

The Majority of Stau2 Target mRNAs Are Localized to Neuronal Processes

Local translation at synapses contributes to several forms of synaptic plasticity (Costa-Mattioli et al., 2009; Sutton and Schuman, 2006). Recent data indicate that 2,550 mRNAs localize to the processes of CA1 neurons in the hippocampus (Cajigas et al., 2012). According to those data, 3,508 transcripts were expressed in these cells, therefore suggesting that ~72% of all RNAs in the CA1 processes may be locally translated. To determine the number of Stau2 target mRNAs in this local pool, we cross-referenced our data set with that of Cajigas et al. (2012) (Table S3). Approximately 30% of the Stau2 targets were expressed in the CA1 somatic layer (Figure 2A). Of these, ~77% were found in the neuropil layer, which consists of neuronal processes (Figure 2A). This is a small but significant enrichment of localized messages in the IP over input, which also consisted of ~72% localized messaged (resampling without replacement, $p = 0.012$). This suggests that the majority of endogenous Stau2 target RNAs localize away from the cell body into neuronal processes. Using fluorescence in situ hybridization (FISH), we further confirmed the localization of two Stau2 targets of interest, *Rgs4* and *Calm3*, to dendrites of primary rat hippocampal neurons (Figure 2B). Thus, Stau2 may play a role in dendritic localization of its target mRNAs.

Stau2 Regulates mRNA Levels in Primary Neurons

To elucidate the role of Stau2 on the regulation of target mRNAs in primary neurons, we investigated the impact of Stau2 downregulation on global gene expression. Primary cortical neurons were transduced with lentivirus vectors expressing short hairpin RNAs (shRNAs), which target Stau2 or a control hairpin (targeting luciferase). After 5 days, total RNA was isolated and differences in gene expression were identified by microarray from three independent experiments. When Stau2 levels were reduced to ~10% of endogenous levels, 349 target mRNAs were downregulated and 99 upregulated (Figure 3A, lane 3; Figure 3B; Table S4). Interestingly, however, when a less potent shRNA was used, resulting in 30% of Stau2 remaining (shStau2-v3; Figure 3A, lane 4), the levels of only 13 RNAs changed (Figure S2A), with Stau2 itself being the only common target. These results suggest that

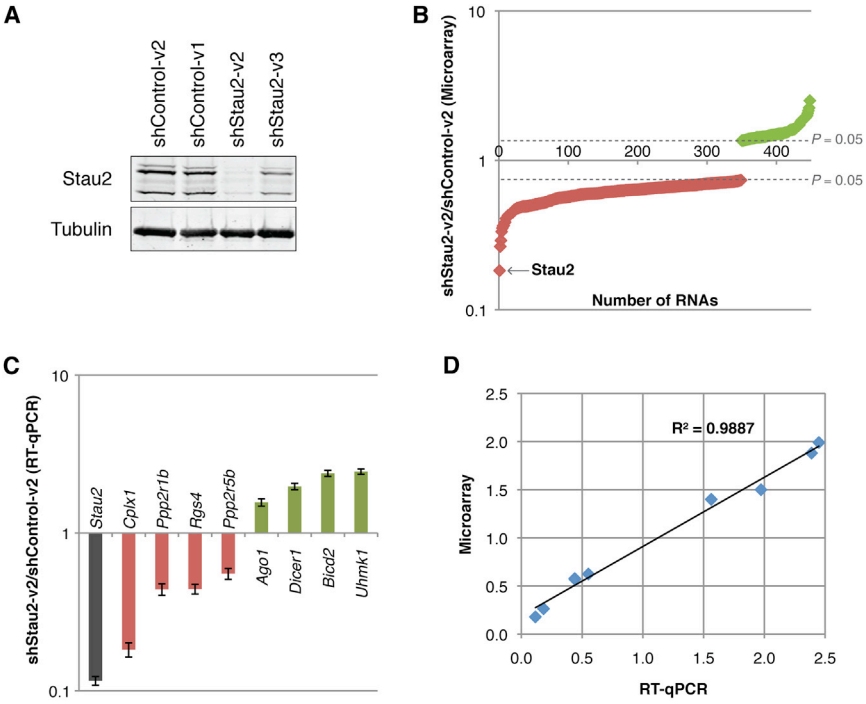

Figure 3. Stau2 Regulates mRNA Levels in Primary Neurons

(A) Western blot from primary cortical neurons transduced with lentivirus expressing two independent shRNAs targeting Stau2 or controls (2 + 5 DIV). Four isoforms of Stau2 (62, 59, 56, and 52 kDa) are expressed. Tubulin was used as loading control.

(B) Microarray analysis was performed on total RNA isolated from shStau2-v2 and shControl-v2 transduced primary cortical neurons. Significantly changed mRNAs are ordered by fold change in the knockdown relative to the control. Each dot represents a single mRNA, with red showing downregulated mRNAs and green showing upregulated mRNAs. Stau2 is indicated because it was the most downregulated RNA.

(C) qRT-PCR validation of eight mRNAs from the microarray. Relative levels of the indicated RNAs were determined in the shStau2-v2 knockdown relative to the control, shControl-v2, using cross-normalization to the reference genes *Kif5c* and *PPIA*. Bars represent the mean ± SEM (n = 3).

(D) Correlation between the validated targets shown in (C) and the fold change for the same targets according to the microarray (Pearson's correlation coefficient, $p < 0.001$).

(E and F) GO terms enrichments ($p < 0.05$) for significantly downregulated (E) and upregulated (F) mRNAs following Stau2 downregulation (KD) in cortical neurons (shStau2-v2). Benjamini-Hochberg (BH) adjusted p values are shown.

See also Figure S2 and Table S4.

E RNAs DOWN-regulated in Stau2 KD:

Term	No. of RNAs	*P*-value (BH)
Synapse part	18	5.76E-04
Dendrite	16	1.57E-03
Neuron projection	22	1.59E-03
Synapse	20	1.78E-03
Learning or memory	13	2.53E-03
Plasma membrane	65	3.37E-03
Behavior	22	4.39E-03
Synaptic vesicle	8	1.56E-02
Plasma membrane	41	1.58E-02
Cell projection	26	2.14E-02

F RNAs UP-regulated in Stau2 KD:

Term	No. of RNAs	*P*-value (BH)
Serine/threonine-protein kinase	6	2.03E-02
ATP-binding	10	2.50E-02
Kinase	8	4.75E-02

30% of normal Stau2 levels are sufficient to maintain target mRNA levels in primary neurons. The microarray data were again validated by qRT-PCR, showing a high correlation between both data sets (Figures 3C, 3D, S2B, and S2C). Interestingly, the downregulated RNAs were enriched for "synaptic" and "learning and memory"-related GO term categories, whereas the upregulated ones were enriched for different GO terms (Figures 3E and 3F). Together, gene expression analysis shows that the majority of target genes identified are downregulated in Stau2 knockdown neurons.

Identification of a Staufen-Recognized Structure in Downregulated Stau2 Targets

In order to further investigate how Stau2 might regulate specific transcripts in the brain, we searched for structural elements enriched in Stau2 targets. Here, we took advantage of our two independent microarray experiments to select the most stringent set of targets. Specifically, we selected those mRNAs that were enriched in the IP of endogenous Stau2 RNPs from rat brain, which were also affected by Stau2 downregulation in primary neurons. This resulted in 32 targets whose levels decreased in the absence of Stau2 and 6 that increased (Figure 4A; Table S5). Interestingly, and in line with what was recently reported for *Drosophila* Staufen targets (Laver et al., 2013), the median length of the 3′ UTRs of Stau2-regulated targets was significantly greater than that in the rat 3′ UTRome (1,189 bases for targets versus 496 bases for the rat 3′ UTRome, Wilcoxon rank sum $p < 0.0001$; Figure 4B). We next took advantage of a novel computational strategy that was recently used to identify structural elements in *Drosophila* Staufen target RNAs (Laver et al., 2013) to assess whether the Stau2 targets were enriched for Staufen-recognized structures (SRSs) similar to those in *Drosophila*. We found that the Stau2 target 3′ UTRs were highly enriched for Type III SRSs (Wilcoxon rank sum $p < 0.001$; Figure 4C). Type III SRSs are defined by a stem consisting of at least 10 out of 12 paired bases and no more than two "unpaired" bases (i.e., those that participate in neither canonical nor noncanonical base pairings) (Laver et al., 2013). Notably, 95% (19 out of 20) of the analyzed downregulated targets carried one or more Type III SRSs whereas only 33% (one out of three) analyzed upregulated targets contained a type III SRSs (Figure S3; data not shown).

Given that downregulation was the predominant effect of Stau2 knockdown on the target RNAs, we further validated

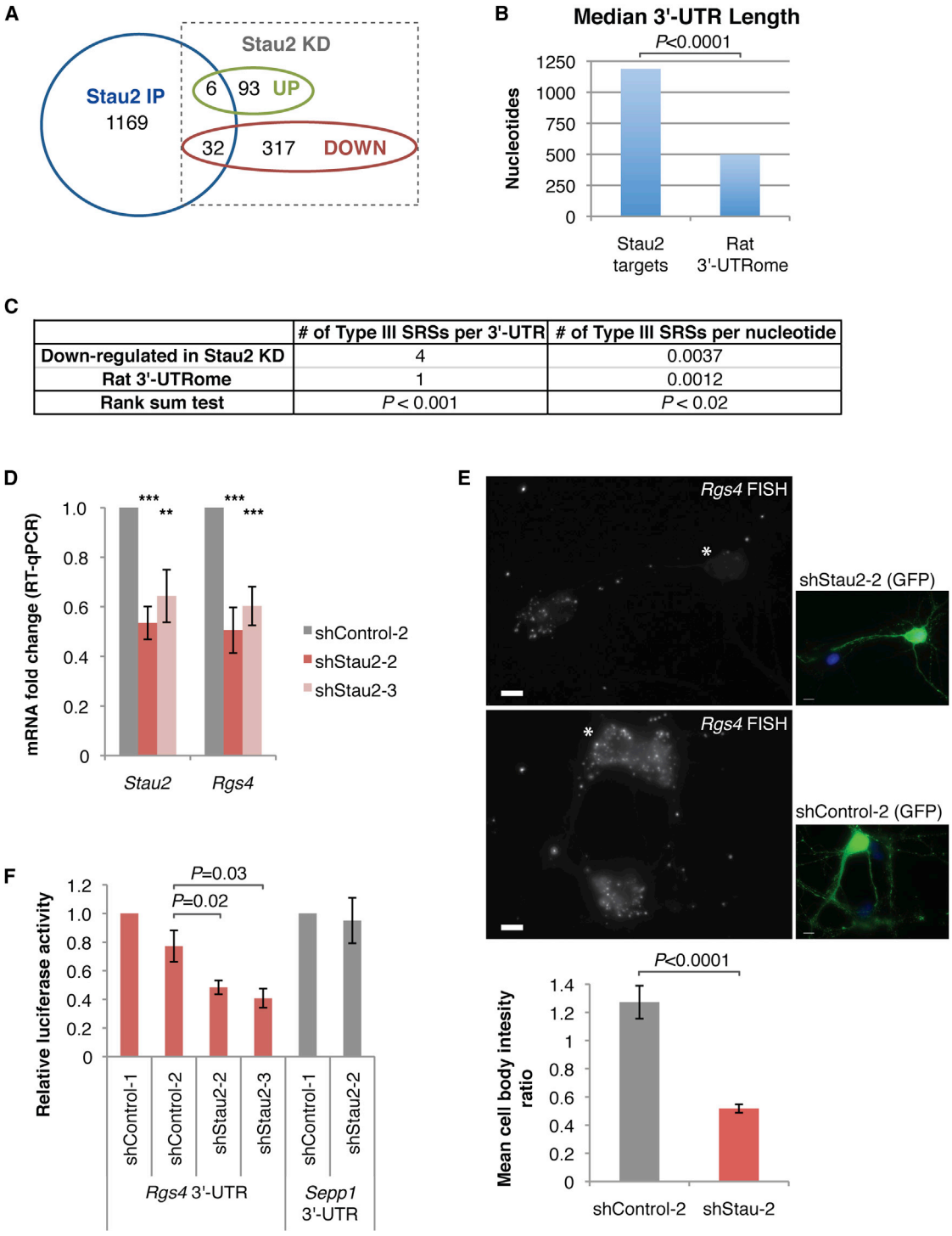

C

	# of Type III SRSs per 3'-UTR	# of Type III SRSs per nucleotide
Down-regulated in Stau2 KD	4	0.0037
Rat 3'-UTRome	1	0.0012
Rank sum test	$P < 0.001$	$P < 0.02$

Figure 4. Stau2-Stabilized Target mRNA 3′ UTRs Are Enriched for Staufen-Recognized Structures

(A) Overlap between mRNAs enriched in the Stau2 IP (from Figure 1) and mRNAs significantly changed following Stau2 knockdown (from Figure 3B). mRNAs changed following the Stau2 knockdown (KD) are separated into upregulated (green circle) and downregulated (red circle).

(B) Median 3′ UTR length of Stau2-regulated targets (overlap shown in A) compared to the rat genome. Note that only 23 of the 38 targets shown in (A) could be used for this analysis due to incomplete database entries for the remainder (see Experimental Procedures). $p < 0.0001$, Wilcoxon rank sum test.

(C) Type III Staufen-recognized structures (SRSs) were mapped in the 3′ UTRs of Stau2 targets and nontargets. The average number of Type III SRSs per transcript and the frequency of SRSs are shown, both of which were significantly different between Stau2 targets (n = 20) and the rat 3′ UTRome (n = 11,775). Wilcoxon rank sum test p values are shown.

(legend continued on next page)

one target, the regulator of G protein signaling 4 (*Rgs4),* which is one of the synaptic mRNAs of the GPCR pathway and was reduced by both Stau2 shRNAs to a statistically significant level (reduced by 49% and 40% with shStau2-2 and shStau2-3, respectively; Figure 4D). Note that shStau2-3 produces a stronger knockdown when nucleofection or calcium transfection was used, as compared to the viral-mediated knockdown shown earlier (Figures S4A–S4C). The *Rgs4* mRNA 3′ UTR (*ENSRNOG0000002773* in Figure S3A) contains two Type III SRSs. This effect was further validated at the single-cell level using *Rgs4* FISH following Stau2 downregulation with shStau2-2 (Figure 4E) and shStau2-3 (data not shown), where the effect was even more stark (Student's t test $p < 0.0001$). Since there was almost no *Rgs4* left in the processes of Stau2-downregulated neurons, only the cell body levels could be quantified.

To determine whether the observed reduction of *Rgs4* mRNA upon Stau2 knockdown is mediated via its 3′ UTR, we generated an *Rgs4* 3′ UTR luciferase reporter and performed luciferase assays in cortical neurons. Consistent with the reduction in endogenous *Rgs4* RNA we observed upon Stau2 knockdown, *Rgs4* reporter expression significantly decreased upon Stau2 downregulation with both shRNAs (Figure 4F). Together with the qRT-PCR results, these findings suggest that Stau2 stabilizes the *Rgs4* mRNA via it's 3′ UTR.

CONCLUSIONS AND OUTLOOK

Here, we sought to identify physiologically relevant Stau2 targets using a combined approach of immunoprecipitation of Stau2-associated RNAs (to identify targets) together with the effect of downregulation on those targets (to identify the role of Stau2 in posttranscriptional regulation of these targets). While other studies have identified candidate Stau2 targets, we found very little overlap with our data set (Figure S4D), most likely because the earlier studies did not fractionate Stau2-containing particles away from ER. We believe that the more stringent approach described here has yielded several insights into Stau2 function.

First, we have provided evidence for a role of Stau2 in the stabilization of mRNAs as Stau2 targets were predominantly downregulated in Stau2-deficient neurons. We note that the levels of a small fraction of Stau2 targets increase upon Stau2 downregulation, consistent with a recent study in human cell lines that implicates Stau2 in transcript destabilization (Park et al., 2013). Although no such role of transcript stabilization has been reported for Stau2 before, there is a recent publication for Stau1, together with the long noncoding RNA TINCR, showing a role in stabilizing differentiation mRNAs in human keratinocytes (Kretz et al., 2013).

Second, our computational analysis of the Stau2 targets suggests that it recognizes targets via secondary structures similar to those that *Drosophila* Staufen recognizes in the 3′ UTRs of its targets (Laver et al., 2013). Given that the *Rgs4* 3′-UTR contains two such secondary structures (Type III SRSs) and together with our finding that a reporter RNA carrying the *Rgs4* 3′-UTR behaves similarly to endogenous *Rgs4* mRNA upon Stau2 knockdown, this supports the hypothesis that Stau2 regulates its target RNAs by binding to type III SRSs in their 3′ UTRs. Thus, the secondary structures recognized by Staufen family proteins may be conserved from flies to mammals.

Third, given that *Rgs4* is a synaptic signaling molecule and Stau2 downregulation has previously described synaptic phenotypes (Goetze et al., 2006; Lebeau et al., 2011), misregulation of *Rgs4* following Stau2 knockdown could provide a mechanism for the observed phenotypes. It is of particular note that Rgs4 has been linked to neuropsychiatric disorders (Terzi et al., 2009), the stress response (Ni et al., 1999), and is responsive to antidepressant drugs (Stratinaki et al., 2013). Therefore, regulation by Stau2 would be of wide interest not only in the field of RNA biology but also in clinical neurosciences.

Finally, it is very likely that mammalian Staufen proteins act as multifunctional posttranscriptional regulators (St Johnston, 2005). In neurons, Stau2 likely plays a role in mRNA localization, stability, and translation. Here, we focused on its effects on mRNA regulation, uncovering a novel function in the stabilization of steady-state levels of synaptic target RNAs, thus providing a link between the molecular role of Stau2 as an RBP and its cellular functions at the synapse.

EXPERIMENTAL PROCEDURES

Immunoprecipitations, RNA Isolation, and qRT-PCR

IPs were performed as described in RNase-free conditions on ice (Fritzsche et al., 2013). RNA was isolated directly from beads and subjected to qRT-PCR or microarray analysis in a minimum of three independent experiments.

Microarrays

For IP microarray analysis, RNA (200 ng) from input or IP was used for identifying Stau2-associated RNAs. Preparation of terminal-labeled cDNA, hybridization to genome-wide GeneChip Rat Gene 1.0 ST Array (Affymetrix) and scanning of the arrays were carried out according to manufacturer's protocols (https://www.affymetrix.com). Each IP as well as RNA isolated from the input sample was analyzed from three biological replicates. Microarray data were

(D) qRT-PCR of *Stau2* and *Rgs4* mRNAs following knockdown of Stau2 in cortical neurons. Differences in steady-state RNA levels between shControl and shStau2 samples were determined using the $\Delta\Delta C_T$ method and cross-normalization to the reference genes *PPIA*, *Arntl*, and *Vinculin*. Bars represent mean change ± SEM (n = 5). Significant differences were determined between shStau2 and shControl samples using the Student's t test. $^{**}p < 0.01$, $^{***}p < 0.001$.
(E) *Rgs4* FISH in primary hippocampal neurons following knockdown of Stau2. The 8 DIV neurons were transfected with the indicated shRNA and fixed 4 days later for FISH. Antisense RNA probes were used to detect endogenous *Rgs4* mRNA and GFP antibodies to detect shRNA-transfected cells. Transfected cells are indicated with an asterisk in the FISH image. Note that some bleed-through from the GFP staining leads to a diffuse signal in the FISH channel, which also slightly underestimates differences in the quantification. Average cell body intensity of *Rgs4* FISH signal was quantified from transfected cells and normalized to neighboring untransfected cells. Bars represent the mean ratio of transfected to untransfected cells ± SEM taken from three independent experiments (shControl-2, n = 25; shStau2-2, n = 25). Scale bar, 10 μM.
(F) Dual luciferase reporter assay in cortical neurons. Renilla activity was normalized to Firefly to control for transfection efficiency. This ratio was then normalized to shControl-1 and the luciferase empty vector. Bars represent the mean relative luciferase activity ± SEM ($n \geq 4$). *Sepp1* is an unaffected Stau2-enriched mRNA. p values were calculated using the Student's t test.
See also Figures S3 and S4 and Tables S5 and S6.

analyzed with the R/BioConductor suite (http://www.bioconductor.org). Robust multiarray analysis was used for normalization (Irizarry et al., 2003). A linear model was used for inferring differential expression between groups (Smyth, 2004). p values were adjusted using the Benjamini-Hochberg method (Benjamini and Hochberg, 1995). For knockdown microarrays, the GeneChip Rat Gene 2.0 ST Array (Affymetrix) was used. The experiment and analysis were performed as described above.

FISH and Immunocytochemistry

FISH using tyramide signal amplification was performed as described previously (Vessey et al., 2008). The following RNA probes were used: Calm3 sense and antisense from EST IMAGp998L0619945Q (accession number AF231407), 1.3 kb from the 3′ UTR of Calm3; Rgs4 (accession number NM_017214) antisense probe in the first 1 kb of the 3′ UTR, sense probe in the last 1.3 kb of the 3′ UTR. Immunocytochemistry was performed as previously described (Zeitelhofer et al., 2008). Images were acquired using an Axioplan microscope (Zeiss) with a 63× planApo oil-immersion objective, 1.40 NA, and an F-view II charge-coupled device camera (Olympus). For FISH following Stau2 knockdown, 8 days in vitro (DIV) primary hippocampal neurons were transfected using calcium phosphate and fixed at 12 DIV. Images were acquired using an Observer Z1 microscope (Zeiss) with a 63× planApo oil-immersion objective, 1.40 NA, and an CoolSnap HQ2 camera (Olympus). Quantification of average cell body intensity was carried out using Zen (Zeiss). An equal number of transfected and untransfected cells from each coverslip (from three independent experiments) were quantified and the ratio of transfected to untransfected used to determine differences between shStau2 and shControl cells.

Antibodies

Monospecific Stau2 and Barentsz rabbit polyclonal antibodies were generated in our laboratory by affinity purification from existing immune sera: Staufen2 antibodies were directed against the 62 kDa isoform of mouse Stau2 (Zeitelhofer et al., 2008), and anti-Btz antibodies were directed against the C terminus of Btz (amino acids 356–527) (Macchi et al., 2003). The following commercial antibodies were used: anti-phospho ERK1/2 (Cell Signaling Technologies, 4370), anti-ERK1/2 (Cell Signaling Technologies, 4696), anti-Tubulin (Sigma, clone B512) and anti-Vinculin (Santa Cruz, sc-7649).

Primary Neuron Culture

Embryonic day 17 (E17) hippocampal neurons were isolated from embryos of timed pregnant Sprague-Dawley rats (Charles River Laboratories) as previously described (Goetze et al., 2006). Dissociated primary cortical neurons were prepared from cortices remaining from hippocampal dissections. See Supplemental Experimental Procedures for more information.

Lentivirus Production

For lentivirus production, HEK293-FT were transiently cotransfected with psPAX2, pVSVg, and the shRNA constructs using Lipofectamine 2000 (Invitrogen). Supernatants were concentrated by ultracentrifugation (22,000 rpm, 2 hr, SW28 rotor; Beckman Coulter). Virus particles were resuspended in Neurobasal medium (Life Technologies). Neurons were transduced on day 2 and collected on day 5 for analysis (DIV 2+5).

Computational Analysis of Staufen Target 3′ UTRs

We downloaded *Rattus norvegicus* (Rnor_5.0) cDNA sequences from Ensembl using BioMart in August 2013 and defined 3′ UTRs as the portion of the cDNA 3′- to the open reading frame, as defined by Ensembl. When there were multiple isoforms for a gene, we used the longest isoform to represent its mature mRNA sequence. Then, to identify SRSs in these 3′ UTRs, we followed our previously described protocol (Laver et al., 2013). See Supplemental Experimental Procedures for details.

Luciferase Assay

Gene fragments of interest were cloned downstream of the Renilla luciferase gene into the psiCHECK-2 vector (Promega). As control, empty luciferase reporter plasmid was used. Rat primary cortical neurons (E17–E18) were transfected with 5 μg of reporter plasmid and 25 μg of shRNA plasmid into 1.2 × 10^6 cells and then distributed into six wells of a 24-well plate. Luciferase assays were performed after 3 days using the Dual-Luciferase Reporter Assay System (Promega) according to the manufacturer's instructions using the GloMax device (Promega). Ratios of Renilla/Firefly luciferase activity were calculated and normalized to the shControl and the luciferase empty vector. The mean of the normalized ratio from three or more independent experiments was used to determine significant differences with the Student's t test.

Further details are available in Supplemental Experimental Procedures.

SUPPLEMENTAL INFORMATION

Supplemental information includes Supplemental Experimental Procedures, four figures, and six tables and can be found with this article online at http://dx.doi.org/10.1016/j.celrep.2013.11.039.

ACKNOWLEDGMENTS

We thank Christin Illig and Marco Tolino for assistance with preparation of primary neuron cultures, Daniela Karra for initial work involving RNA isolation for microarrays, and Dorothee Dormann, Marija Vukajlovic, and Jernej Ule for comments on the manuscript. This work was supported by the Austrian Science Fund (P20583-B12, I 590-B09, SFB F43), the ESF Program RNAQuality (I 127-B12), the Schram Foundation and an HFSP network grant (RGP24/2008) (all to M.A.K.), and Canadian Institutes of Health Research operating grants (MOP-125894 to Q.D.M. and MOP-14409 to H.D.L.). J.H. was supported by a PhD fellowship from the FWF (DK RNA Biology: W1207-B09). D.E. was supported by the Helmholtz Young Investigator program (HZ-NG-607).

Received: June 3, 2013
Revised: November 4, 2013
Accepted: November 21, 2013
Published: December 19, 2013

REFERENCES

Benjamini, Y., and Hochberg, Y. (1995). Controlling the false discovery rate: a practical and powerful approach to multiple testing. J. R. Stat. Soc. Series B Stat. Methodol. *57*, 289–300.

Cajigas, I.J., Tushev, G., Will, T.J., tom Dieck, S., Fuerst, N., and Schuman, E.M. (2012). The local transcriptome in the synaptic neuropil revealed by deep sequencing and high-resolution imaging. Neuron *74*, 453–466.

Costa-Mattioli, M., Sossin, W.S., Klann, E., and Sonenberg, N. (2009). Translational control of long-lasting synaptic plasticity and memory. Neuron *61*, 10–26.

Darnell, J.C., Van Driesche, S.J., Zhang, C., Hung, K.Y., Mele, A., Fraser, C.E., Stone, E.F., Chen, C., Fak, J.J., Chi, S.W., et al. (2011). FMRP stalls ribosomal translocation on mRNAs linked to synaptic function and autism. Cell *146*, 247–261.

Dubnau, J., Chiang, A.S., Grady, L., Barditch, J., Gossweiler, S., McNeil, J., Smith, P., Buldoc, F., Scott, R., Certa, U., et al. (2003). The staufen/pumilio pathway is involved in Drosophila long-term memory. Curr. Biol. *13*, 286–296.

Dugré-Brisson, S., Elvira, G., Boulay, K., Chatel-Chaix, L., Mouland, A.J., and DesGroseillers, L. (2005). Interaction of Staufen1 with the 5′ end of mRNA facilitates translation of these RNAs. Nucleic Acids Res. *33*, 4797–4812.

Fritzsche, R., Karra, D., Bennett, K., Ang, F.Y., Heraud-Farlow, J., Tolino, M., Doyle, M., Bauer, K.E., Thomas, S., Planvavsky, M., et al. (2013). Interactome of two diverse RNA granules links mRNA localization to translational repression in neurons. Cell Rep. *5*, this issue, 1749–1762.

Goetze, B., Tuebing, F., Xie, Y., Dorostkar, M.M., Thomas, S., Pehl, U., Boehm, S., Macchi, P., and Kiebler, M.A. (2006). The brain-specific double-stranded RNA-binding protein Staufen2 is required for dendritic spine morphogenesis. J. Cell Biol. *172*, 221–231.

Hogan, D.J., Riordan, D.P., Gerber, A.P., Herschlag, D., and Brown, P.O. (2008). Diverse RNA-binding proteins interact with functionally related sets of RNAs, suggesting an extensive regulatory system. PLoS Biol. *6*, e255.

Holt, C.E., and Bullock, S.L. (2009). Subcellular mRNA localization in animal cells and why it matters. Science *326*, 1212–1216.

Huang, W., Sherman, B.T., and Lempicki, R.A. (2009). Systematic and integrative analysis of large gene lists using DAVID bioinformatics resources. Nat. Protoc. *4*, 44–57.

Irizarry, R.A., Bolstad, B.M., Collin, F., Cope, L.M., Hobbs, B., and Speed, T.P. (2003). Summaries of Affymetrix GeneChip probe level data. Nucleic Acids Res. *31*, e15.

Kandel, E.R. (2009). The biology of memory: a forty-year perspective. J. Neurosci. *29*, 12748–12756.

Keene, J.D. (2007). RNA regulons: coordination of post-transcriptional events. Nat. Rev. Genet. *8*, 533–543.

Kim, Y.K., Furic, L., Desgroseillers, L., and Maquat, L.E. (2005). Mammalian Staufen1 recruits Upf1 to specific mRNA 3'UTRs so as to elicit mRNA decay. Cell *120*, 195–208.

Köhrmann, M., Luo, M., Kaether, C., DesGroseillers, L., Dotti, C.G., and Kiebler, M.A. (1999). Microtubule-dependent recruitment of Staufen-green fluorescent protein into large RNA-containing granules and subsequent dendritic transport in living hippocampal neurons. Mol. Biol. Cell *10*, 2945–2953.

Kretz, M., Siprashvili, Z., Chu, C., Webster, D.E., Zehnder, A., Qu, K., Lee, C.S., Flockhart, R.J., Groff, A.F., Chow, J., et al. (2013). Control of somatic tissue differentiation by the long non-coding RNA TINCR. Nature *493*, 231–235.

Laver, J.D., Li, X., Ancevicius, K., Westwood, J.T., Smibert, C.A., Morris, Q.D., and Lipshitz, H.D. (2013). Genome-wide analysis of Staufen-associated mRNAs identifies secondary structures that confer target specificity. Nucleic Acids Res. *41*, 9438–9460.

Lebeau, G., Miller, L.C., Tartas, M., McAdam, R., Laplante, I., Badeaux, F., DesGroseillers, L., Sossin, W.S., and Lacaille, J.C. (2011). Staufen 2 regulates mGluR long-term depression and Map1b mRNA distribution in hippocampal neurons. Learn. Mem. *18*, 314–326.

Lin, K., Wang, D., and Sadée, W. (2002). Serum response factor activation by muscarinic receptors via RhoA. Novel pathway specific to M1 subtype involving calmodulin, calcineurin, and Pyk2. J. Biol. Chem. *277*, 40789–40798.

Macchi, P., Kroening, S., Palacios, I.M., Baldassa, S., Grunewald, B., Ambrosino, C., Goetze, B., Lupas, A., St Johnston, D., and Kiebler, M. (2003). Barentsz, a new component of the Staufen-containing ribonucleoprotein particles in mammalian cells, interacts with Staufen in an RNA-dependent manner. J. Neurosci. *23*, 5778–5788.

Micklem, D.R., Adams, J., Grünert, S., and St Johnston, D. (2000). Distinct roles of two conserved Staufen domains in oskar mRNA localization and translation. EMBO J. *19*, 1366–1377.

Miura, M., Watanabe, M., Offermanns, S., Simon, M.I., and Kano, M. (2002). Group I metabotropic glutamate receptor signaling via Galpha q/Galpha 11 secures the induction of long-term potentiation in the hippocampal area CA1. J. Neurosci. *22*, 8379–8390.

Ni, Y.G., Gold, S.J., Iredale, P.A., Terwilliger, R.Z., Duman, R.S., and Nestler, E.J. (1999). Region-specific regulation of RGS4 (Regulator of G-protein-signaling protein type 4) in brain by stress and glucocorticoids: in vivo and in vitro studies. J. Neurosci. *19*, 3674–3680.

Park, E., Gleghorn, M.L., and Maquat, L.E. (2013). Staufen2 functions in Staufen1-mediated mRNA decay by binding to itself and its paralog and promoting UPF1 helicase but not ATPase activity. Proc. Natl. Acad. Sci. USA *110*, 405–412.

Rashid, A.J., So, C.H., Kong, M.M., Furtak, T., El-Ghundi, M., Cheng, R., O'Dowd, B.F., and George, S.R. (2007). D1-D2 dopamine receptor heterooligomers with unique pharmacology are coupled to rapid activation of Gq/11 in the striatum. Proc. Natl. Acad. Sci. USA *104*, 654–659.

Smyth, G.K. (2004). Linear models and empirical bayes methods for assessing differential expression in microarray experiments. Stat. Appl. Genet. Mol. Biol. *3*, Article3.

St Johnston, D., Beuchle, D., and Nüsslein-Volhard, C. (1991). Staufen, a gene required to localize maternal RNAs in the Drosophila egg. Cell *66*, 51–63.

St Johnston, D. (2005). Moving messages: the intracellular localization of mRNAs. Nat. Rev. Mol. Cell Biol. *6*, 363–375.

Stratinaki, M., Varidaki, A., Mitsi, V., Ghose, S., Magida, J., Dias, C., Russo, S.J., Vialou, V., Caldarone, B.J., Tamminga, C.A., et al. (2013). Regulator of G protein signaling 4 [corrected] is a crucial modulator of antidepressant drug action in depression and neuropathic pain models. Proc. Natl. Acad. Sci. USA *110*, 8254–8259.

Sutton, M.A., and Schuman, E.M. (2006). Dendritic protein synthesis, synaptic plasticity, and memory. Cell *127*, 49–58.

Tang, S.J., Meulemans, D., Vazquez, L., Colaco, N., and Schuman, E. (2001). A role for a rat homolog of staufen in the transport of RNA to neuronal dendrites. Neuron *32*, 463–475.

Terzi, D., Stergiou, E., King, S.L., and Zachariou, V. (2009). Regulators of G protein signaling in neuropsychiatric disorders. Prog. Mol. Biol. Transl. Sci. *86*, 299–333.

Ule, J., Ule, A., Spencer, J., Williams, A., Hu, J.S., Cline, M., Wang, H., Clark, T., Fraser, C., Ruggiu, M., et al. (2005). Nova regulates brain-specific splicing to shape the synapse. Nat. Genet. *37*, 844–852.

Vessey, J.P., Macchi, P., Stein, J.M., Mikl, M., Hawker, K.N., Vogelsang, P., Wieczorek, K., Vendra, G., Riefler, J., Tübing, F., et al. (2008). A loss of function allele for murine Staufen1 leads to impairment of dendritic Staufen1-RNP delivery and dendritic spine morphogenesis. Proc. Natl. Acad. Sci. USA *105*, 16374–16379.

Zeitelhofer, M., Karra, D., Macchi, P., Tolino, M., Thomas, S., Schwarz, M., Kiebler, M., and Dahm, R. (2008). Dynamic interaction between P-bodies and transport ribonucleoprotein particles in dendrites of mature hippocampal neurons. J. Neurosci. *28*, 7555–7562.

Zimyanin, V.L., Belaya, K., Pecreaux, J., Gilchrist, M.J., Clark, A., Davis, I., and St Johnston, D. (2008). In vivo imaging of oskar mRNA transport reveals the mechanism of posterior localization. Cell *134*, 843–853.